Proceedings of Symposia in Applied Mathematics

On the entropy stability of Roe-type finite volume methods

Mária Lukáčová - Medviďová and Eitan Tadmor

Abstract. We study the entropy stability of a class of finite volume (FV) methods for systems of hyperbolic conservation laws. The methods under consideration are based on a Roe-type linearization coupled with the multidimensional FV evolution Galerkin method [**8**]. Following Tadmor [**16**] we derive the second-order numerical viscosity which guarantees the entropy stability of these Roe-type FV schemes. Numerical experiments confirm that the resulting schemes have just the right amount of numerical viscosity: small enough to retain sharp shock profiles, yet large enough to enforce a correct resolution of sonic rarefactions.

1. Introduction

In this paper we consider a class of finite volume methods for nonlinear conservation laws, based on a suitable Roe-type linearization method coupled with the finite volume evolution Galerkin (FVEG) schemes.

Since the former method is classical [**13**] and widely used in the literature, we will describe here more closely only the latter one. The finite volume evolution Galerkin (FVEG) methods belong to the class of genuinely multidimensional finite volume scheme, see, e.g., [**6**]-[**9**]. They couple a finite volume formulation with approximate evolution operators which are based on the theory of bi-characteristics for the first order systems [**6**]. As a result, exact integral equations for linear or linearized hyperbolic conservation laws can be derived, which take into account all of the infinitely many directions of wave propagation.

In the finite volume framework, the approximate evolution operators are used to evolve the computed solution at $t = t^n$, along the cell interfaces, up to an intermediate time level $t^{n+\frac{1}{2}}$, in order to compute fluxes. This step can be considered as a predictor step. In the corrector step the finite volume update is done. Extensive numerical experiments confirm robustness, good multidimensional behavior, high accuracy, stability, and efficiency of the FVEG schemes, see, e.g. [**7**]-[**9**].

1991 *Mathematics Subject Classification.* 65L05, 65M06, 35L45, 35L65, 65M25, 65M15.

Key words and phrases. systems of hyperbolic conservation laws, finite volume evolution Galerkin schemes, the Roe scheme, entropy stability, entropy conservative schemes, semi-discrete conservative schemes.

This research has been done during the sabbatical stay of the first author at the CSCAMM, University of Maryland. She would like to acknowledge the hospitality of the CSCAMM. Research was supported in part by NSF grant 07-07949 and ONR grant N00014-91-J-1076.

In this paper we investigate *entropy stability* of the FVEG schemes for one-dimensional systems. We follow the works of Tadmor [**15**]-[**17**] and study the entropy stability of FVEG schemes using the comparison approach with the so-called *entropy conservative* schemes. Further results on entropy-stable/entropy-conservative schemes can be found in [**1, 3, 5, 12, 18**] and in the references therein.

Entropy analysis presented here illustrates the role of entropy-stable flux function and indicates that in order to keep the FVEG scheme entropy-stable an entropy correction term measuring jumps in the wave speeds corresponding to rarefaction waves has to be added. We present only a brief overview of main theoretical results, a detailed analysis will be given elsewhere [**10**]. Our main focus is to demonstrate entropy stable behavior of the resulting scheme by means of numerical experiments. Indeed, it has just the right amount of numerical viscosity: small enough to retain sharp shock profiles and yet large enough to get a correct resolution of sonic rarefactions.

2. Entropy-conservative and entropy-stable schemes

We consider the one-dimensional system of hyperbolic conservation laws,

$$\frac{\partial}{\partial t}\boldsymbol{u}+\frac{\partial}{\partial x}\boldsymbol{f}(\boldsymbol{u})=0, \tag{2.1}$$

governing the N-vector of conserved variables $\boldsymbol{u}:=[u_1,\cdots,u_N]^\top:\mathbb{R}\times\mathbb{R}^+\to\mathbb{R}^N$ and balanced by the flux functions $\boldsymbol{f}(u):=[f_1,\cdots,f_N]^\top\in C^1(\mathbb{R}^N,\mathbb{R}^N)$. We assume it is endowed with an entropy pair, (U,F), such that every strong solution of (2.1) satisfies the entropy equality

$$\frac{\partial}{\partial t}U(\boldsymbol{u})+\frac{\partial}{\partial x}F(\boldsymbol{u})=0, \tag{2.2a}$$

whereas weak solutions are sought to satisfy the *entropy inequality*

$$\frac{\partial}{\partial t}U(\boldsymbol{u})+\frac{\partial}{\partial x}F(\boldsymbol{u})\le 0, \tag{2.2b}$$

For simplicity, we assume that the Jacobian matrix, $\boldsymbol{A}(u):=\boldsymbol{f}_{\boldsymbol{u}}(\boldsymbol{u})$ is *symmetric*, with real eigenvalues, $\lambda^j\equiv\lambda^j(\boldsymbol{A})$, $\lambda^1\le\lambda^2\le\ldots\le\lambda^N$. We note in passing that the assumption of symmetry is not a restriction, since by change of variables, $\boldsymbol{u}\to\boldsymbol{v}:=U_{\boldsymbol{u}}(\boldsymbol{u})$, one obtains the desired symmetry of the *equivalent* system, e.g., [**16**, section 2]

$$\frac{\partial}{\partial t}\boldsymbol{u}(\boldsymbol{v})+\frac{\partial}{\partial x}\boldsymbol{f}(\boldsymbol{u}(\boldsymbol{v}))=0,$$

where $\boldsymbol{u}_{\boldsymbol{v}}(\boldsymbol{v})$ and $\boldsymbol{f}_{\boldsymbol{v}}(\boldsymbol{u}(\boldsymbol{v}))$ are symmetric.

We now turn our attention to consistent approximations of (2.1),(2.2b), based on semi-discrete finite volume (FV) methods of the form

$$\frac{\mathrm{d}}{\mathrm{d}t}\boldsymbol{u}_\nu(t)+\frac{\boldsymbol{H}_{\nu+\frac12}-\boldsymbol{H}_{\nu-\frac12}}{\Delta x_\nu}=0. \tag{2.3}$$

Here, $\boldsymbol{u}_\nu(t)$ denotes the discrete solution along the grid lines, (x_ν,t), which consists of cells of variable size, $\Delta x_\nu:=x_{\nu+\frac12}-x_{\nu-\frac12}$ centered at $x_\nu=\big(x_{\nu+\frac12}+x_{\nu-\frac12}\big)/2$, and

$$\boldsymbol{H}_{\nu+\frac12}:=\boldsymbol{H}\left(\boldsymbol{u}_\nu(t),\boldsymbol{u}_{\nu+1}(t)\right)$$

is the numerical flux which approximates the physical one, $\boldsymbol{H}_{\nu+\frac{1}{2}} \approx \boldsymbol{f}(\boldsymbol{u}(x_{\nu+\frac{1}{2}}))$ at the cell interface $(x_{\nu+\frac{1}{2}}, t)$; in particular, $\boldsymbol{H}$ is consistent with $\boldsymbol{f}$ so that $\boldsymbol{H}(\boldsymbol{u}, \boldsymbol{u}) = \boldsymbol{f}(\boldsymbol{u})$.

We say that the finite volume schemes (2.3) are *entropy-stable* if the following cell-entropy inequality, analogous to (2.2a), holds

$$\frac{\mathrm{d}}{\mathrm{d}t}U(\boldsymbol{u}_\nu(t)) + \frac{F_{\nu+\frac{1}{2}} - F_{\nu-\frac{1}{2}}}{\Delta x_\nu} \leq 0; \tag{2.4}$$

here $U(\boldsymbol{u})$ is the convex entropy function and $F_{\nu+\frac{1}{2}} := F\left(\boldsymbol{u}_\nu(t), \boldsymbol{u}_{\nu+1}(t)\right)$ is the corresponding consistent entropy flux function such that $F(\boldsymbol{u}, \boldsymbol{u}) = F(\boldsymbol{u})$. From (2.4) it follows that the total amount of entropy $\sum U(\boldsymbol{u}_\nu(t))\Delta x_\nu$ does not increase in time, which is the apriori energy estimate sought for nonlinear semi-discrete schemes (2.3). In the particular case that equality takes place in (2.4), analogous to (2.2b),

$$\frac{\mathrm{d}}{\mathrm{d}t}U(\boldsymbol{u}_\nu(t)) + \frac{F_{\nu+\frac{1}{2}} - F_{\nu-\frac{1}{2}}}{\Delta x_\nu} = 0, \tag{2.5}$$

we say that the FV scheme (2.3) is *entropy-conservative*, following Tadmor [**16**].

The discrete formulation can be generalized to the non-symmetric case where the numerical solution is sought in terms of the discrete entropy variables, $\boldsymbol{u}_\nu(t) \to \boldsymbol{u}(\boldsymbol{v}_\nu(t))$; consult [**16**].

3. Entropy stability and viscosity form

In this section we consider a special class of the finite volume schemes which are based on a suitable linearization of the corresponding Riemann problem. Using the local entropy analysis along the corresponding (approximate) Riemann paths in phase space proposed in [**16**], we will show, using a comparison principle, that these schemes are entropy-stable.

A path in phase space. Consider two neighboring discrete values $\boldsymbol{u}_\nu$ and $\boldsymbol{u}_{\nu+1}$. We now describe the construction of a general path in phase space connecting $\boldsymbol{u}_\nu$ to $\boldsymbol{u}_{\nu+1}$, along an *arbitrary* set of linearly independent system $\boldsymbol{r}_+ := \{\boldsymbol{r}^j_{\nu+\frac{1}{2}}\}_{j=1,\ldots,N}$; $|\,\boldsymbol{r}^j_{\nu+\frac{1}{2}}\,| = 1$. To this end, let $\boldsymbol{\ell}_+ := \{\boldsymbol{\ell}^j_{\nu+\frac{1}{2}}\}_{j=1,\ldots,N}$, be the corresponding orthogonal system $\langle \boldsymbol{r}^j_+, \boldsymbol{\ell}^k_+ \rangle = \delta_{jk}$. Starting at $\boldsymbol{u}^1_+ := \boldsymbol{u}_\nu$, we will follow with the intermediate states, $\boldsymbol{u}^2_+, \ldots,$

$$\boldsymbol{u}^{j+1}_+ = \boldsymbol{u}^j_+ + \alpha^j_+ \boldsymbol{r}^j_+, \qquad j = 1, \ldots, N, \tag{3.1a}$$

ending with $\boldsymbol{u}^{N+1}_+ = \boldsymbol{u}_{\nu+1}$. Here, the α's,

$$\alpha^j_+ := \left\langle \boldsymbol{\ell}^j_+, \Delta\boldsymbol{u}_+ \right\rangle, \qquad \Delta\boldsymbol{u}_+ := \boldsymbol{u}_{\nu+1} - \boldsymbol{u}_\nu, \tag{3.1b}$$

measure the strength of the waves along the different sub-paths. The passage from $\boldsymbol{u}_\nu = \boldsymbol{u}^1_+$ to the state on its right $\boldsymbol{u}_{\nu+1} = \boldsymbol{u}^{N+1}_+$ is now made of sub-paths, $\boldsymbol{u}^j_+(\xi)$, connecting $\boldsymbol{u}^j_+$ to $\boldsymbol{u}^{j+1}_+$, which are conveniently parameterized over the symmetric interval $-1/2 \leq \xi \leq 1/2$,

$$\boldsymbol{u}^j_+(\xi) : \left[-\frac{1}{2}, \frac{1}{2}\right] \mapsto \{\boldsymbol{u}^j_+, \boldsymbol{u}^{j+1}_+\}. \tag{3.1c}$$

The specific construction of these sub-paths, $\boldsymbol{u}_+ = \{\boldsymbol{u}_+^j(\xi)\}_{j=1,\dots,N}$, is at our disposal. As an example, we quote from [**16**, section 6] the piecewise linear path

$$\boldsymbol{u}_\pm^j(\xi) = \frac{1}{2}\left(\boldsymbol{u}_\pm^j + \boldsymbol{u}_\pm^{j+1}\right) + \xi\alpha_\pm^j \boldsymbol{r}_\pm^j, \quad \frac{1}{2} \le \xi \le \frac{1}{2}, \qquad j = 1, \dots, N; \tag{3.2}$$

we have used here an analogous notation for the left cell interface between $\boldsymbol{u}_{\nu-1}$ and $\boldsymbol{u}_\nu$.

Using these paths $\boldsymbol{u}_\pm(\xi)$, we can now formulate the following general comparison argument for entropy stability.

THEOREM 3.1 (Tadmor [**16**]). *Consider the semi-discrete scheme,*

$$\begin{aligned} \frac{d}{dt}\boldsymbol{u}_\nu(t) = \; - \; & \frac{1}{2\Delta x_\nu}\left[\sum_{j=1}^N \left\langle \boldsymbol{f}\left(\boldsymbol{u}_+^j\right) + \boldsymbol{f}\left(\boldsymbol{u}_+^{j+1}\right), \boldsymbol{r}_+^j \right\rangle \boldsymbol{\ell}_+^j \right. \\ & \left. - \sum_{j=1}^N \left\langle \boldsymbol{f}\left(\boldsymbol{u}_-^j\right) + \boldsymbol{f}\left(\boldsymbol{u}_-^{j+1}\right), \boldsymbol{r}_-^j \right\rangle \boldsymbol{\ell}_-^j \right] \\ + \; & \frac{1}{2\Delta x_\nu}\left[\sum_{j=1}^N q_+^j\, \alpha_+^j\, \boldsymbol{\ell}_+^j - \sum_{j=1}^N q_-^j\, \alpha_-^j \boldsymbol{\ell}_-^j\right], \end{aligned} \tag{3.3}$$

where, $q_\pm = \{q_\pm^j\}_{j=1}^N$ are arbitrary numerical viscosity amplitudes at our disposal.

(i) [Entropy conservation]. *The scheme (3.3) is entropy conservative if the numerical viscosities, $q_\pm = q_\pm^*$, are chosen as*

$$q_\pm^{*,j} := \begin{cases} \dfrac{1}{\alpha_\pm^j}\displaystyle\int_{-\frac{1}{2}}^{\frac{1}{2}} 2\xi \left\langle \boldsymbol{A}\left(\boldsymbol{u}_\pm^j(\xi)\right)\frac{d\boldsymbol{u}_\pm^j(\xi)}{d\xi}, \boldsymbol{r}_\pm^j \right\rangle d\xi & \text{if } \alpha_\pm^j \neq 0, \\ 0 & \text{if } \alpha_\pm^j = 0. \end{cases} \tag{3.4}$$

(ii) [Comparison]. *The semi-discrete scheme (3.3) is entropy stable if it contains more numerical viscosity than the entropy conservative scheme (3.3),(3.4), namely*

$$q_\pm^j \ge q_\pm^{*,j}. \tag{3.5}$$

REMARK 3.2. The viscosity term (3.4) is path independent and is left at our disposal. If we choose $\boldsymbol{u}_\pm(\xi)$ to be the *piecewise linear* path (3.2), then the entropy conservative viscosity (3.4) amounts to

$$q_\pm^{*,j} = \int_{-\frac{1}{2}}^{\frac{1}{2}} 2\xi \left\langle \boldsymbol{A}\left(\boldsymbol{u}_\pm^j(\xi)\right)\boldsymbol{r}_\pm^j, \boldsymbol{r}_\pm^j \right\rangle d\xi, \qquad \boldsymbol{u}_\pm^j(\xi) := \frac{1}{2}\left(\boldsymbol{u}_\pm^j + \boldsymbol{u}_\pm^{j+1}\right) + \xi\alpha_\pm^j \boldsymbol{r}_\pm^j, \tag{3.6}$$

which is the entropy conservative scheme introduced in [**16**, corollary 6.2]. Theorem 3.1 generalizes the framework of entropy stability outlined in [**16**].

Using the comparison approach outlined in theorem 3.1, we turn to study the entropy stability of semi-discrete FV schemes, by comparing its numerical viscosity vs. an entropy conservative numerical viscosity. To this end, we have to specify

our choice of the path in phase-space and the amount of numerical viscosity along this path.

4. The FVEG scheme and its viscosity form along shock-based path

We study now the entropy stability, or in fact the lack of it in difference schemes based on shock paths. We connect the sub-paths $\{\boldsymbol{u}_+^j(\xi)\}_{j=1}^N$, through *shock waves* such that

(4.1)
$$\boldsymbol{f}\left(\boldsymbol{u}_+^j(\xi)\right) - \boldsymbol{f}\left(\boldsymbol{u}_+^j\right) = s_+^j(\xi)\left(\boldsymbol{u}_+^j(\xi) - \boldsymbol{u}_+^j\right), \quad \boldsymbol{u}_+^j(-\frac{1}{2}) = \boldsymbol{u}_+^j, \quad j = 1, \ldots, N.$$

Set $\boldsymbol{u}_+^{j+1} - \boldsymbol{u}_+^j = \alpha_+^j \boldsymbol{r}_+^j$. Thus, we resolve the interface between $\boldsymbol{u}_\nu$ and $\boldsymbol{u}_{\nu+1}$ through a series of shocks and (4.1) at $\xi = 1/2$ are nothing but the corresponding Rankine-Hugoniot conditions

$$\boldsymbol{f}\left(\boldsymbol{u}_+^{j+1}\right) - \boldsymbol{f}\left(\boldsymbol{u}_+^j\right) = s_+^j\left(\boldsymbol{u}_+^{j+1} - \boldsymbol{u}_+^j\right), \quad j = 1, \ldots, N, \tag{4.2}$$

ordered by their increasing scalar speeds, $\{s_+^j \equiv s_+^j(\boldsymbol{u}_+^j(\xi = 1/2))\}$, $s_+^1 \le s_+^2 \le \ldots \le s_+^N$. We know, [**4**], that such a path exists, at least "in the small", $\|\Delta \boldsymbol{u}_+\| \ll 1$. But such a path does not necessarily yield entropy stability; only the compressive shocks, for which $\mathrm{d}s_+^j(\xi)/\mathrm{d}\xi < 0$ are admissible.

We now focus our attention on the class of one-dimensional FV schemes which will be sought in connection with the *multidimensional FVEG methods*. To guarantee their entropy stability, we employ the numerical fluxes

$$\boldsymbol{H}_{\nu+\frac{1}{2}} = \boldsymbol{H}(\boldsymbol{u}_\nu, \boldsymbol{u}_{\nu+1}) := \boldsymbol{f}(\boldsymbol{u}^*_{\nu+\frac{1}{2}}) - \mathcal{J}_{\nu+\frac{1}{2}}, \tag{4.3a}$$

which involves the intermediate state $\boldsymbol{u}^*_{\nu+\frac{1}{2}} \equiv \boldsymbol{u}^*_+$,

$$\boldsymbol{u}^*_+ := \boldsymbol{u}_\nu + \sum_{\{j:\ s_+^j \le 0\}} \alpha_+^j \boldsymbol{r}_+^j, \tag{4.3b}$$

and an entropy correction term, $\mathcal{J}_{\nu+\frac{1}{2}} \equiv \mathcal{J}_+$, given by

$$\mathcal{J}_+ := \frac{\kappa}{2}\sum_{j=1}^N \left[\lambda_+^j\right]^+ \alpha_+^j \boldsymbol{r}_+^j, \qquad \left[\lambda_+^j\right]^+ = \max\{\lambda_+^j, 0\}. \tag{4.3c}$$

Here, κ is an amplitude to be tuned later on, and $\left[\lambda_+^j\right]^+$ is the *positive part*[1] of the jumps across the sub-paths,

$$\left[\lambda_+^j\right] := \lambda^j\left(\boldsymbol{A}(\boldsymbol{u}_+^{j+1})\right) - \lambda^j\left(\boldsymbol{A}(\boldsymbol{u}_+^j)\right). \tag{4.3d}$$

To verify the entropy stability of (4.3), we will utilize the entropy stability framework of Theorem 3.1, and to this end we need to compute the viscosity coefficients associated with the FVEG scheme (4.3). This is the content of our next result.

[1]We denote by $x^+ = \max\{x, 0\}$ and $x^- = \min\{x, 0\}$ the positive and negative parts of x.

LEMMA 4.1. *Consider the shock-based path* $\left\{\boldsymbol{u}_+^j\right\}_{j=1\dots N+1}$, *such that (4.2) holds. Then the FVEG scheme (4.3) admits the standard viscosity form*

$$\begin{aligned}\frac{d}{dt}\boldsymbol{u}_\nu(t) &= -\frac{1}{2\Delta x_\nu}\Big[\boldsymbol{f}\left(\boldsymbol{u}_{\nu+1}\right)-\boldsymbol{f}\left(\boldsymbol{u}_{\nu-1}\right)\Big]\\ &\quad+\frac{1}{2\Delta x_\nu}\left[\sum_{j=1}^{N} q_+^j\,\alpha_+^j\,\boldsymbol{\ell}_+^j-\sum_{j=1}^{N} q_-^j\,\alpha_-^j\boldsymbol{\ell}_-^j\right]\end{aligned}\tag{4.4}$$

with viscosity coefficients

$$q_+^j=\left|s_+^j\right|+\kappa\left[\lambda_+^j\right]^+.\tag{4.5}$$

Assuming additionally that $\left\{\boldsymbol{r}_+^j\right\}_{j=1,\dots,N+1}$ *are orthonormal then the center flux difference can be rewritten in the following form, cf. (3.3),*

$$\begin{aligned}\frac{1}{2\Delta x_\nu}\Big[\boldsymbol{f}(\boldsymbol{u}_{\nu+1})-\boldsymbol{f}(\boldsymbol{u}_{\nu-1})\Big]=\frac{1}{2\Delta x_\nu}\Bigg[&\sum_{j=1}^{N}\left\langle\boldsymbol{f}\left(\boldsymbol{u}_+^j\right)+\boldsymbol{f}\left(\boldsymbol{u}_+^{j+1}\right),\boldsymbol{r}_+^j\right\rangle\boldsymbol{\ell}_+^j\\ &-\sum_{j=1}^{N}\left\langle\boldsymbol{f}\left(\boldsymbol{u}_-^j\right)+\boldsymbol{f}\left(\boldsymbol{u}_-^{j+1}\right),\boldsymbol{r}_-^j\right\rangle\boldsymbol{\ell}_-^j\Bigg].\end{aligned}\tag{4.6}$$

PROOF. Derivation of (4.6) can be found in [**10**]. Note also that even if the shock-based path is not orthogonal (4.6) holds in the higher order terms.

Now, in order to prove (4.4) let us assume that there are k negative eigenvalues $s_+^j\le 0$. The choice of u_+^* in (4.3b) yields

$$\begin{aligned}\boldsymbol{f}(\boldsymbol{u}_\nu)-\boldsymbol{f}(\boldsymbol{u}_+^*) &\equiv \boldsymbol{f}(\boldsymbol{u}_+^1)-\boldsymbol{f}(\boldsymbol{u}_+^k)=-\sum_{j=1}^{k-1}\boldsymbol{f}(\boldsymbol{u}_+^{j+1})-\boldsymbol{f}(\boldsymbol{u}_+^j)\\ &= -\sum_{j=1}^{k-1} s_+^j\;\alpha_+^j\;\boldsymbol{r}_+^i=-\sum_{j=1}^{N}\left(s_+^j\right)^-\;\alpha_+^j\;\boldsymbol{r}_+^j.\end{aligned}\tag{4.7}$$

Similarly, $\boldsymbol{f}(\boldsymbol{u}_{\nu+1})-\boldsymbol{f}(\boldsymbol{u}_+^*)=\sum_{j=1}^{N}\left(s_+^j\right)^+\;\alpha_+^j\;\boldsymbol{r}_+^j$.
Averaging the last two equations we find

$$\frac{1}{2}\Big(\boldsymbol{f}(\boldsymbol{u}_\nu)+\boldsymbol{f}(\boldsymbol{u}_{\nu+1})\Big)=\boldsymbol{f}(\boldsymbol{u}_+^*)+\frac{1}{2}\sum_{j=1}^{N}\left|s_+^j\right|\alpha_+^j\;\boldsymbol{r}_+^j.$$

Thus, the numerical flux of the FVEG schemes (4.3a), $\boldsymbol{f}(\boldsymbol{u}_+^*)-\mathcal{J}_+$, equals

$$\begin{aligned}\boldsymbol{H}(\boldsymbol{u}_\nu,\boldsymbol{u}_{\nu+1}) &= \frac{1}{2}\Big(\boldsymbol{f}(\boldsymbol{u}_\nu)+\boldsymbol{f}(\boldsymbol{u}_{\nu+1})\Big)-\frac{1}{2}\sum_{j=1}^{N}\left|s_+^j\right|\alpha_+^j\;\boldsymbol{r}_+^j-\mathcal{J}_+\\ &= \frac{1}{2}\Big(\boldsymbol{f}(\boldsymbol{u}_\nu)+\boldsymbol{f}(\boldsymbol{u}_{\nu+1})\Big)-\frac{1}{2}\sum_{j=1}^{N}\Big(\left|s_+^j\right|+\kappa\left[\lambda_+^j\right]^+\Big)\alpha_+^j\;\boldsymbol{r}_+^j.\end{aligned}\tag{4.8}$$

Plugging (4.8) in the standard FV formulation (2.3) we conclude with the desired form of the q's in (4.5). □

The viscosity form (4.4), (4.5) of our FVEG will enable us to fine-tune the amount of numerical viscosities $q_\pm$ along the corresponding waves to enforce entropy stability. In particular, the analysis presented below yields an entropy stability condition for appropriately large entropy amplitude κ.

5. The entropy stability of FVEG schemes

The aim of this section is to verify, whether the estimate (3.5) holds for the FVEG scheme (2.3), (4.3). Actually, we will be able to show that the inequality (3.5) holds to the leading order term. However, the numerical experiments presented in the next section demonstrate that the effect of the higher order terms is negligible. The jump term J_+ proposed in (4.3c) in fact yields numerical schemes which correctly resolve typical entropy-type problems, such as the correct resolution of the sonic rarefaction.

Let us firstly formulate the main result of this section.

THEOREM 5.1. *Consider the mid-value Jacobian, $\overline{\boldsymbol{A}}^{j+\frac{1}{2}}$, evaluated at the subpaths $\boldsymbol{u}_+$,*

$$\overline{\boldsymbol{A}}^{j+\frac{1}{2}} := \boldsymbol{A}(\boldsymbol{u}_+^j(0)), \qquad \boldsymbol{u}_+^j(0) = \frac{1}{2}(\boldsymbol{u}_+^j + \boldsymbol{u}_+^{j+1}).$$

Let $\left\{\overline{\boldsymbol{r}}^k_{j+\frac{1}{2}}\right\}_{k=1}^N$ be the right orthonormal eigenvectors of $\overline{\boldsymbol{A}}^{j+\frac{1}{2}}$, with the corresponding eigenvalues of $\overline{\boldsymbol{A}}^{j+\frac{1}{2}}$.

We assume that the following condition holds.

$$|\overline{\boldsymbol{r}}^j_{j+\frac{1}{2}} - \boldsymbol{r}^j_+| + |\overline{\lambda}^j_{j+\frac{1}{2}} - s^j_+| \le c|\Delta \boldsymbol{u}_+|^2. \tag{5.1}$$

Then setting the entropy constant $\kappa \ge 1/4$ we have

$$q_+^{*,j} \le q_+^j + c|\Delta \boldsymbol{u}_+|^2. \tag{5.2}$$

PROOF. We will outline here only the main idea of proof, further details can be found in [**10**]. In order to illustrate derivation of the jump term $\mathcal{J}_+$, cf. (4.3c), we will show that the following property holds

$$\int_{-\frac{1}{2}}^{\frac{1}{2}} 2\xi \left\langle \boldsymbol{A}\left(\boldsymbol{u}_+^j(\xi)\right) \boldsymbol{r}^j(\boldsymbol{u}_+^j(\xi)), \boldsymbol{r}^j(\boldsymbol{u}_+^j(\xi))\right\rangle \mathrm{d}\xi \le \frac{1}{4}\left[\lambda_+^j\right]^+, \tag{5.3}$$

where $\boldsymbol{r}^j(\boldsymbol{u}_+^j)$ is the normalized right eigenvector of the matrix $\boldsymbol{A}(\boldsymbol{u}_+^j)$.
Indeed, we have

$$\int_{-\frac{1}{2}}^{\frac{1}{2}} 2\xi \left\langle \boldsymbol{A}\left(\boldsymbol{u}_+^j(\xi)\right) \boldsymbol{r}^j(\boldsymbol{u}_+^j(\xi)), \boldsymbol{r}^j(\boldsymbol{u}_+^j(\xi))\right\rangle \mathrm{d}\xi = \int_{-\frac{1}{2}}^{\frac{1}{2}} 2\xi\lambda^j\left(\boldsymbol{u}_+^j(\xi)\right)|\boldsymbol{r}^j(\boldsymbol{u}_+^j(\xi))|^2 \mathrm{d}\xi. \tag{5.4}$$

Now, integration by parts and the normalization $|\boldsymbol{r}^j(\boldsymbol{u}_+^j(\xi))| = 1$ yield

$$\int_{-\frac{1}{2}}^{\frac{1}{2}} 2\xi\lambda^j\left(\boldsymbol{u}_+^j(\xi)\right)|\boldsymbol{r}^j(\boldsymbol{u}_+^j(\xi))|^2 \mathrm{d}\xi = \int_{-\frac{1}{2}}^{\frac{1}{2}} \left(\frac{1}{4} - \xi^2\right)\frac{\mathrm{d}}{\mathrm{d}\xi}\lambda^j(\boldsymbol{u}_+^j(\xi))\,\mathrm{d}\xi. \tag{5.5}$$

There are two possible scenarios. In the case of an admissible shock discontinuity, $\lambda^j(\boldsymbol{u}_+^j(\xi))$ is decreasing across the shock path and the integral on the right becomes negative: entropy is dissipated and no additional numerical viscosity is required. In

the case of a rarefaction wave, $\mathrm{d}\lambda^j(\boldsymbol{u}^j_+)/\mathrm{d}\xi > 0$ and additional numerical viscosity is required to prevent "expansive shocks". According to the comparison principle in theorem 5.1, a sufficient amount of numerical viscosity is given by the following upper bound of (5.5)

$$\int_{-\frac{1}{2}}^{\frac{1}{2}} \left(\frac{1}{4} - \xi^2\right) \frac{\mathrm{d}}{\mathrm{d}\xi}\lambda^j(\boldsymbol{u}^j_+(\xi))\mathrm{d}\xi \le \frac{1}{4}\left[\lambda^j_+\right]^+. \tag{5.6}$$

Thus, choosing $\kappa \ge \frac{1}{4}$ the right hand side is bounded by q^j_+, cf. (4.5). □

Remark 5.2. We should point out that in our practical implementation of the FVEG scheme the local linearization is done by freezing the corresponding Jacobian matrix in the local average $\boldsymbol{u}_\pm$. Thus, from the viewpoint of the entropy analysis the orthonormal system $\{\boldsymbol{r}^j_\pm\}_{j=1}^N$ corresponds to the right eigenvectors of the exact mid-value Jacobian $\boldsymbol{A}(\boldsymbol{u}_\pm)$. Analogous results have been obtained using the Roe matrix. The reliability of the correction term J, which is indicated by the numerical analysis above, will be confirmed by the set of numerical experiments in the next section.

6. Numerical experiments

Consider the homogeneous shallow water equations written in conservative variables

$$\partial_t \boldsymbol{u} + \partial_{x_1} \boldsymbol{f}_1(\boldsymbol{u}) + \partial_{x_2} \boldsymbol{f}_2(\boldsymbol{u}) = 0, \tag{6.1}$$

with

$$\boldsymbol{u} := \begin{pmatrix} h \\ hu \\ hv \end{pmatrix}, \quad \boldsymbol{f}_1(\boldsymbol{u}) := \begin{pmatrix} hu \\ hu^2 + \frac{1}{2}gh^2 \\ huv \end{pmatrix}, \quad \boldsymbol{f}_2(\boldsymbol{u}) := \begin{pmatrix} hv \\ huv \\ hv^2 + \frac{1}{2}gh^2 \end{pmatrix}.$$

Here h denotes the water depth, u, v are vertically averaged velocity components and g stays for the gravitational acceleration, we set $g = 10$ in our computations. The Froude number is given as $Fr = |\boldsymbol{w}|/c$, where $\boldsymbol{w} := (u, v)$ and $c = \sqrt{g\,h}$ denotes the wave celerity. The shallow flow is called supercritical, critical or sub-critical for $Fr > 1, Fr = 1$, and $Fr < 1$, respectively.

Now, let us consider a one-dimensional channel with two uniform water levels, both at rest, separated by a wall at $x = 0$

$$\begin{array}{llll} h = 0.1, & u = 0, & & |x| \ge 0, \\ h = 1, & u = 0, & & |x| < 0. \end{array} \tag{6.2}$$

The one-dimensional shallow water equations model the wave propagation after the wall collapses. The wave pattern consists of the left propagating depression wave (rarefaction) and the right propagating bore (shock). The computational domain $[-1, 1]$ was divided into 100 mesh cells. Absorbing boundary conditions were implemented by extrapolating both components of the solution.

This problem is a well-known benchmark in order to test whether a numerical solution satisfies entropy inequality, in particular at the sonic rarefaction wave, i.e. when $Fr = 1$. Numerical methods based on an approximate solution of a linearized Riemann problem typically show the entropy glitch at the critical depression wave (the sonic rarefaction). It is the small discontinuity jump, unphysical entropy violating shock, within the depression. This can be seen very well in our experiments, see Figures 1, 2 for the first and second order FVEG methods, respectively. Several

entropy fixes have been proposed in literature in the last decades, see, e.g., Harten and Hyman [**2**].

Results presented in this paper were obtained using the entropy correction term J derived by theoretical analysis of entropy-stable schemes. In all numerical experiments presented here we have used the entropy constant $\kappa = 1/4$ as suggested by the sharp estimate (5.6). In Figures 1, 2 the water depth h as well as the Froude number Fr for the first and second order FVEG schemes are plotted, respectively. In the second order method the minmod limiter was used. Interestingly, in the shallow water model the effects of entropy violation at the sonic rarefaction are quite large. The entropy correction term derived in this paper works in an excellent way. It clearly affects only the sonic rarefaction part, leaving unchanged the resolution of discontinuities as well as the rest of rarefaction wave.

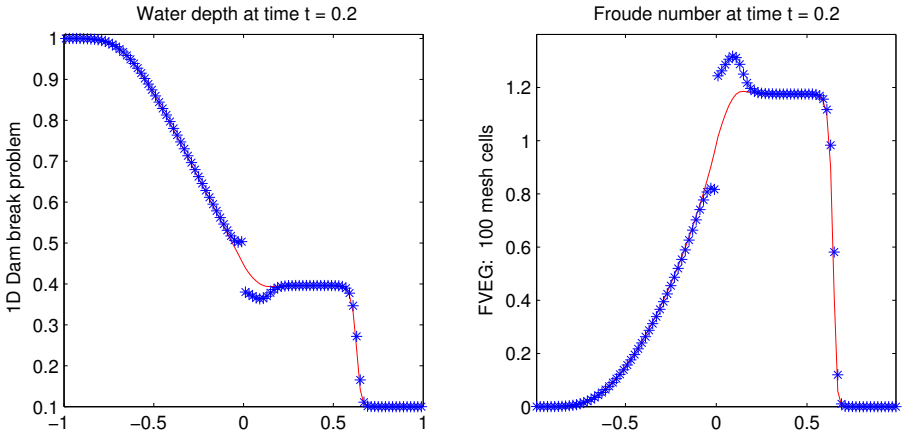

FIGURE 1. Entropy glitch problem in the first order FVEG method; results with entropy correction (solid line), without correction (stars).

References

[1] Crandal M.G., Majda A. Monotone difference approximations for scalar conservation laws. *Math. Comp.* 1980; **34**:1-21.

[2] Harten A., Hyman J.M. Self adjusting grid method for one-dimensional hyperbolic conservation laws. *J. Comput. Phys.* 1983, **50**:235-269.

[3] Khalfallah K., Lerat A., Correction d'entropie pour des schémas numeriques approchant und systéme hyperbolique. *Note CR Acad. Sci.*

[4] Lax, P. D., Hyperbolic systems of conservation laws. II. Comm. Pure Appl. Math. 10 1957 537–566.

[5] LeFloch P., Mercier J.M., Rohde C. Fully discrete, entropy conservative schemes of arbitrary order. *SIAM J. Numer. Anal.* 2002; **40**:1968-1992.

[6] Lukáčová-Medviďová M., Morton K.W., Warnecke G. Evolution Galerkin methods for hyperbolic systems in two space dimensions. *MathComp.* 2000; **69**:1355–1384.

[7] Lukáčová-Medviďová M., Saibertová J., Warnecke G. Finite volume evolution Galerkin methods for nonlinear hyperbolic systems. *J. Comp. Phys.* 2002; **183**:533-562.

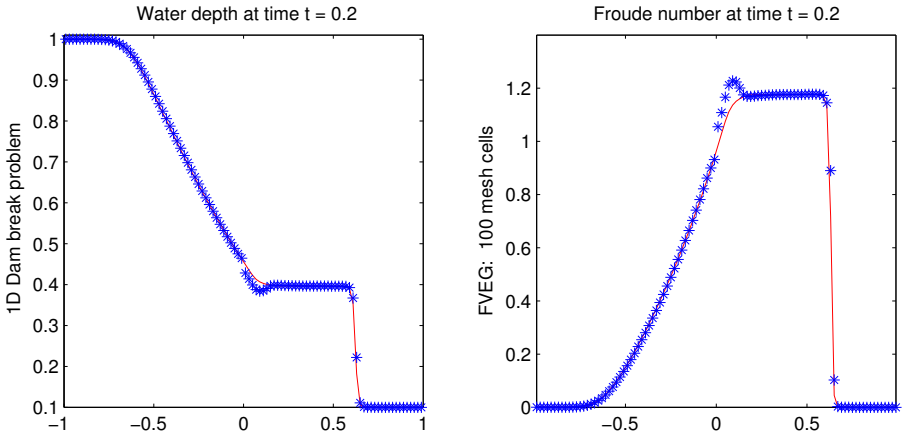

FIGURE 2. Entropy glitch problem in the second order FVEG method; results with entropy correction (solid line), without correction (stars).

[8] Lukáčová-Medviďová M., Morton K.W., Warnecke G. Finite volume evolution Galerkin (FVEG) methods for hyperbolic problems. *SIAM J. Sci. Comput.* 2004; **26(1)**:1-30.

[9] Lukáčová-Medviďová M., Noelle S., Kraft M. Well-balanced finite volume evolution Galerkin schemes for the shallow water equations. *J. Comp. Phys.* 2007; **221**:122-147.

[10] Lukáčová-Medviďová M., Tadmor E. Entropy stability of Roe-type finite volume methods. manuscript, 2008.

[11] Majda A, Osher S., Numerical viscosity and the entropy condition. *Comm. Pure Appl. Math.* 1979; **32**:797-838.

[12] Osher S., Riemann solvers, the entropy condition, and the difference approximations. *SIAM J. Numer. Anal.* 1984; **21**:217-235.

[13] Roe P.L., Approximate Riemann solvers, parameter vectors and difference schemes. *J. Comp. Phys.* 1981; **43**:357-372.

[14] Tadmor E., Numerical viscosity and the entropy condition for conservative difference schemes Math. Comp. 43 (1984), 369-381.

[15] Tadmor E., The numerical viscosity of entropy stable schemes for systems of conservation laws, I. *Math. Comp.* 1987; **49**:91-103.

[16] Tadmor E., Entropy stability theory for difference approximations of nonlinear conservation laws and related time-dependent problems. *Acta Numerica* 2003; 451-512.

[17] Tadmor E., Zhong W., Entropy stable approximation of the Navier-Stokes equations with no artificial numerical viscosity. *J. Hyperbolic. Differ. Equ* 2006; **3(3)**:529-559.

[18] Tadmor E., Zhong W., Energy-preserving and stable approximations for the two-dimensional shallow water equations, in "Mathematics and Computation - A Contemporary View", Proc. of the Third Abel Symposium held in Alesund, Norway May 2006 (H. Munthe-Kaas & B. Owren eds.), Springer 2008.

INSTITUTE OF NUMERICAL SIMULATION, HAMBURG UNIVERSITY OF TECHNOLOGY, SCHWARZENBERGSTRASSE 95, 21079 HAMBURG, GERMANY

E-mail address: lukacova@tu-harburg.de

DEPARTMENT OF MATHEMATICS, INSTITUTE FOR PHYSICAL SCIENCE AND TECHNOLOGY AND CENTER OF SCIENTIFIC COMPUTATION AND MATHEMATICAL MODELING (CSCAMM), UNIVERSITY OF MARYLAND, COLLEGE PARK, MD 20742 USA

E-mail address: tadmor@cscamm.umd.edu